PROCEEDINGS OF SCIENCE

The ATLAS Upgrade Programme

M. Iodice*
INFN Roma Tre
E-mail: mauro.iodice@roma3.infn.it

The Large Hadron Collider (LHC) at CERN offers the best opportunities for exploration of new physics and for precision measurements of known phenomena at the energy frontier. The excellent performance of LHC in 2010-2012 period has proven the ability to deliver luminosity that exceeds expectations and therefore there is an established plan of the accelerator upgrades for higher luminosities, which go well beyond the initial design parameters of the detector.
After a series of upgrades of the complex of the accelerators, during the long shutdown in 2018/ 2019, LHC is expected to reach a peak luminosity of $2-3\times10^{34}\mathrm{cm}^{-2}\mathrm{s}^{-1}$, eventually increasing by a factor 3 in the High-Luminosity LHC era (years 2023 and beyond).
In order to keep the high performance of the detectors under the higher rates, the increased number of multiple interactions per bunch crossing and increase of backgrounds expected with the LHC upgrades, following the LHC schedule, ATLAS has devised a two stage upgrade programme that is summarized in this paper.

INFN Workshop on Future Detectors for HL-LHC,
March 11-13, 2014
Trento, Italy

*Speaker.

PoS(IFD2014)004

1. LHC Upgrade Roadmap and ATLAS Upgrade Plans up to 2030 and beyond.

During the next decades, the Large Hadron Collider (LHC) [1] at CERN has planned a series of upgrades that will substantially increase the instantaneous luminosity beyond its original design parameters. The high energy of LHC and the increase of luminosity offers the best opportunities for exploration of new physics beyond the Standard Model (SM) and for making precision measurements of properties of known phenomena. One of the main objectives of the increase of LHC luminosity is the detailed study of the Higgs boson. With larger luminosity, it will be possible to make precision measurements of its couplings to fermions and bosons, its rare decays and its self-couplings. An increase in luminosity will also allow to extend the range of the searches beyond Standard Model, in particular for SUSY particles, significantly extending the present mass limits.

At the time of this paper, the first long shutdown (LS1 in 2013 – 2014) has just been completed. The repair of the splices in the main accelerator performed during LS1 will allow the LHC to continue its operation close to its design parameters with a center of mass energy of $\sqrt{s} = 13$ TeV, 25 ns bunch spacing and peak luminosities of about $1 \times 10^{34}\text{cm}^{-2}\text{s}^{-1}$, and is expected to deliver an integrated luminosity during RUN–2 of ~ 50 fb^{-1} before the next long shutdown.

The updated planning of the LHC upgrade programme after LS1 has been established at the "Review of LHC and Injector Upgrade Plans" (RLIUP) Meeting [2] in 2013. During the next long shutdown (LS2), starting July 2018 and lasting 18 months, major modifications to the LHC injector complex are envisaged with LHC expected to achieve a peak instantaneous luminosity of about 2×10^{34} cm^{-2}s^{-1} in Run–3 (2020 – 2022). During the third long shutdown (LS3), starting in 2022 for a period of at least 30 months, the LHC will be upgraded to High-Luminosity LHC (HL-LHC). It will provide more populated and denser bunches at the collision regions of the experiments, reaching a nominal levelled instantaneous luminosity of 5×10^{34} cm^{-2}s^{-1} and an "ultimate" design levelled luminosity up to 7×10^{34} cm^{-2}s^{-1} with up to 200 inelastic interactions per bunch crossing (pile-up). In terms of data taking, the goals are to integrate a luminosity of more than 300 fb^{-1} by LS3 moving to RUN–4, after LS3, to an annual integrated luminosities in the range 250-300 fb^{-1} during HL-LHC operation leading to an overall design goal of 3000 fb^{-1} by the mid-2030s.

The LHC experiments face considerable challenges to exploit future increases in luminosity. Following the LHC staged upgrade programme, ATLAS has just completed the "Phase–0" consolidation and maintenance of its subsystems. Ready to start Run–2 operation, ATLAS is also preparing the next phases of upgrade planned for LS2, also referred to as "Phase–I" upgrades as well as for LS3, the "Phase–II" upgrade for HL-LHC.

2. The ATLAS Detector

ATLAS [3] is a general-purpose experiment designed to explore the pp collisions at LHC at center of mass energies up to $\sqrt{s} = 14$ TeV and a maximum peak luminosity of 1×10^{34} cm^{-2}s^{-1}.

The overall ATLAS detector layout is shown in Fig. 1. The inner detector is immersed in a 2 T magnetic field generated by the central solenoid, and is composed by high-resolution semiconductor pixel and strip detectors in the inner part of the tracking volume (PIXel and SCT), and by straw-tube tracking detectors with the capability to generate and detect transition radiation in its outer part (TRT). Among the main intervention during the Phase–0 consolidation work, was the ad-

dition of a fourth layer in the tracking system, the new Insertable B-Layer (IBL) pixel detector [4], now installed and running in the experiment.

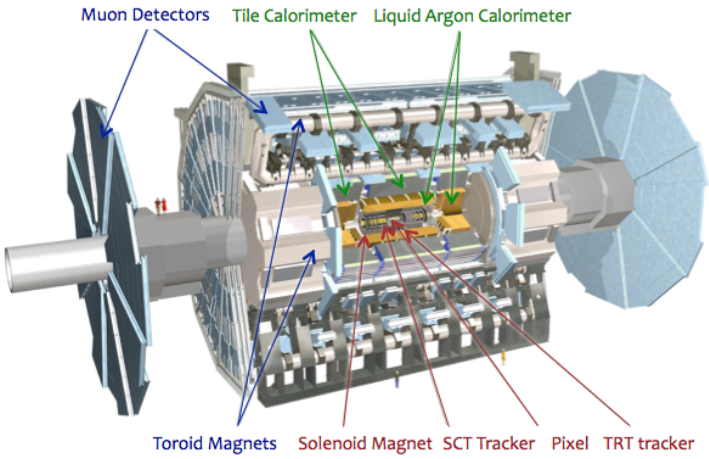

Figure 1: The ATLAS detector.

The calorimeter system is composed by high granularity liquid-argon (LAr) electromagnetic sampling calorimeters covering the pseudorapidity range $|\eta| < 3.2$. The hadronic calorimetry in the range $|\eta| < 1.7$ is provided by a scintillator-tile calorimeter, which is separated into a large barrel and two smaller extended barrel cylinders, one on either side of the central barrel. In the end-caps ($|\eta| > 1.5$), LAr technology is also used for the hadronic calorimeters. The LAr forward calorimeters (FCal) provide both electromagnetic and hadronic energy measurements, and extend the pseudorapidity coverage to $|\eta| = 4.9$.

The muon spectrometer is divided in a central (barrel) and two end-cap regions with a corresponding system of three superconducting toroidal magnets. The azimuthal symmetry of the toroids is reflected in the symmetric structure of the muon chamber system that is subdivided in sixteen sectors (eight large and eight small). In the barrel region, tracks are measured in chambers arranged in three cylindrical layers around the beam axis (inner, middle, outer); in the end-caps, the chambers are installed on three wheels perpendicular to the beam. Over most of the pseudorapidity range ($|\eta| < 2.7$), precision measurements of the track coordinates in the principal bending direction of the magnetic field is provided by Monitored Drift Tubes (MDT), arranged in the three barrel layers and on the three wheels for each end-cap side. Only in the innermost wheels (also referred to as Small Wheel) the Cathode Strip Chambers (CSC) are used to withstand the demanding rate and background conditions ($2.0 < |\eta| < 2.7$). As it will be described, the replacement of the Small Wheels will represent the major upgrade foreseen for Phase–I. The muon trigger system covers the pseudorapidity range $|\eta| < 2.4$. Resistive Plate Chambers (RPC) are used in the barrel (up to $|\eta| < 1.05$) disposed in the middle and outer layers, while in the end-cap regions the trigger is based on the coincidences of the Thin Gap Chambers (TGC) disposed in front and behind the second MDT wheel, also referred to as the Big Wheel.

A three-level trigger system is used to select the events of interest, providing a final average trigger rate of a few hundreds Hz. Each trigger level refines the decisions made at the previous level

and, where necessary, applies additional selection criteria. The ATLAS hardware based Level-1 trigger system (L1) uses inputs from the calorimeter and the muon systems only. Information from the inner detectors is used in the second and third stages of the trigger, collectively referred to as the High Level Trigger (HLT), that executes software algorithms on a large computing farms. The second stage trigger (L2) reconstructs tracks within roads in the tracking system and associates them to objects found in the calorimeter and muon systems with an event processing time of about 40 ms. The final stage of the event selection is carried out by the event filter. Its selections are implemented using offline analysis procedures within an average event processing time of the order of four seconds.

During Run–1 the L1 trigger rates were limited to about 65 kHz, imposed by external constraints (limited bandwidth of some of the detectors) and output rate at HLT were about 300 Hz. One of the main objective of the Phase-I upgrade will be to fully exploit the increase in luminosity and operate efficiently while keeping the trigger thresholds as low as possible. In view of the upcoming Run–2, consolidation works on the detectors and on the Trigger-DAQ system were done in order to keep similar thresholds with respect to Run–1, with an increased L1 rate to about 100 kHz, with a HLT output rate of about 1 kHz.

3. Phase-I ATLAS Upgrade

Driven by the need to keep trigger thresholds as low as possible for detailed studies of the low-mass scale 125 GeV Higgs boson, and at the same time serving the very diverse needs of the searches for beyond standard model physics, the focus of the Phase–I upgrade is to deploy additional means of controlling increasing trigger rates while retaining low p_T lepton thresholds and large acceptances for hadronic and photon trigger objects at L1, and maintaining good selectivity at higher trigger levels.

Detailed plans for Phase–I upgrades are described in [5]. The principal components being:

- The implementation of the Fast Tracker trigger system (FTK) [6], providing tracking information from the inner detector, at start of high-level trigger:
- The new Liquid Argon calorimeter digital trigger chain, for uses of a higher granularity of the system [7];
- The New Small Wheels (NSW) for a much better muon trigger and improved tracking in the endcap regions of the Muon Spectrometer [8];
- The ATLAS Forward Physics (AFP) project, recently approved by the ATLAS Collaboration Board, which will add detectors upstream and downstream ATLAS, at about 210 m from the interaction point, to reconstruct at very forward angle, protons originating from diffractive collisions occurring in ATLAS.

In addition, a range of upgrades to the central Trigger/DAQ system [9] to utilize the above upgrades, and to exploit topological information at L1 are planned, along with other smaller projects for the Muon Spectrometer.

3.1 Fast Tracker (FTK)

The Fast TracKer trigger, (FTK) [6] is a highly parallel hardware system for the trigger upgrade to perform global track reconstruction after each L1 trigger to enable the L2 trigger to have early access to tracking information. FTK will use data from the pixel and semiconductor tracker detectors as well as from the new Insertable B-Layer (IBL) pixel detector and operates in two stages. The first stage is based on associative memories to match the hits in the silicon detectors to 10^9 pre-stored patterns. The second stage consists of fast linear fitting in FPGAs for matched tracks using the hit information in the silicon detectors yielding precise track information. Despite the very short execution time, the FTK reconstructed tracks have a very good quality, similar to the offline quality. FTK exploits the silicon detector full resolution and its tracks can be used for refined b-jet and tau-jet tagging at very high rates, up to 100 kHz (max accepted L1 rate). In Fig. 2-left the transverse impact parameter of tracks associated to light-flavor and heavy-flavor jets is shown, for both the FTK and the offline tracks. The transverse impact parameter distribution is the basic input to b-tagging and a performance of FTK close to the offline reconstruction is reached. In Fig. 2-right the performance of the FTK are shown with respect to the ability to efficiently select jets from b-quarks while providing a large rejection factor against other jets. As can be seen good online rejection can be achieved with little loss in performance.

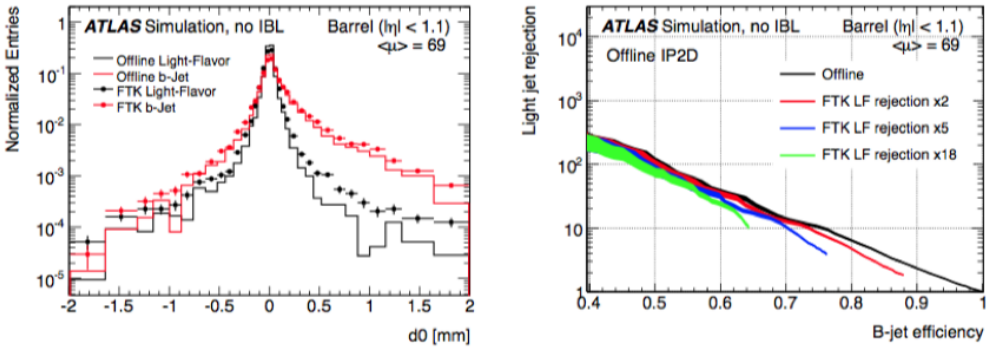

Figure 2: Left: Transverse impact parameter of tracks associated to light-flavor (black) and heavy-flavor (red) jets. Right: Total light-flavor rejection as a function of the total b-jet efficiency. The solid lines show the distribution for the offline tracks, whereas the points show the FTK tracks. The black curve gives the offline performance if no FTK selection is applied, the red, blue and green curves give the performances when a FTK selection is also applied with a light-flavor rejection of 2, 5 and 18, respectively. All simulations shown are for the barrel region and a pile-up of 69 interactions per bunch crossing.

3.2 A finer granularity calorimeter trigger

The objective of the Phase–I upgrade of the Liquid Argon EM calorimeter is to design, build, and install new trigger readout electronics, in order to maintain low p_T thresholds of single and multi-object level-1 calorimeter triggers and improve the electron/jet discrimination. The performance requirements and design specifications of each upgrade component are defined for $\mathscr{L} = 3 \times 10^{34}$ cm^{-2}s^{-1} and 80 interactions per bunch crossing. Such an upgrade of the trigger is fully compatible with Phase–II upgrades 4.3, since it can be considered as a first step of a single, staged

upgrade path. The new electronics, will provide higher-granularity, higher-resolution and longitudinal shower information for he Level-1 trigger processors.

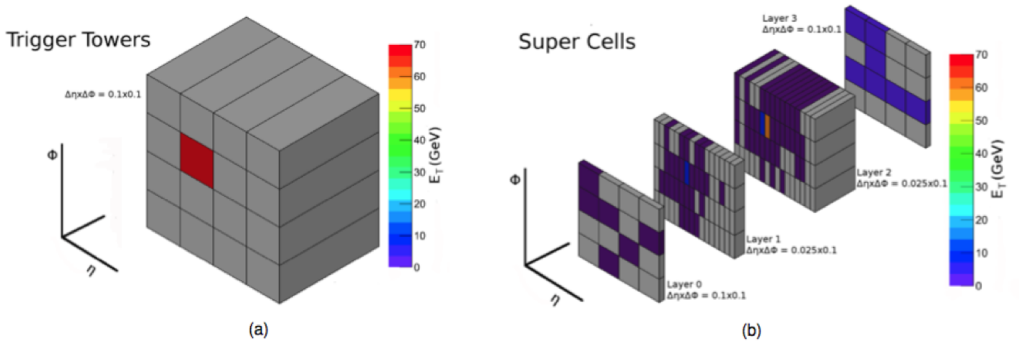

Figure 3: Liquid Argon EM trigger concept and finer granularity proposed for the Phase-I upgrade. An electron (with 70 GeV of transverse energy) as seen by the existing Level-1 Calorimeter trigger electronics (a) and by the proposed upgraded trigger electronics (b).

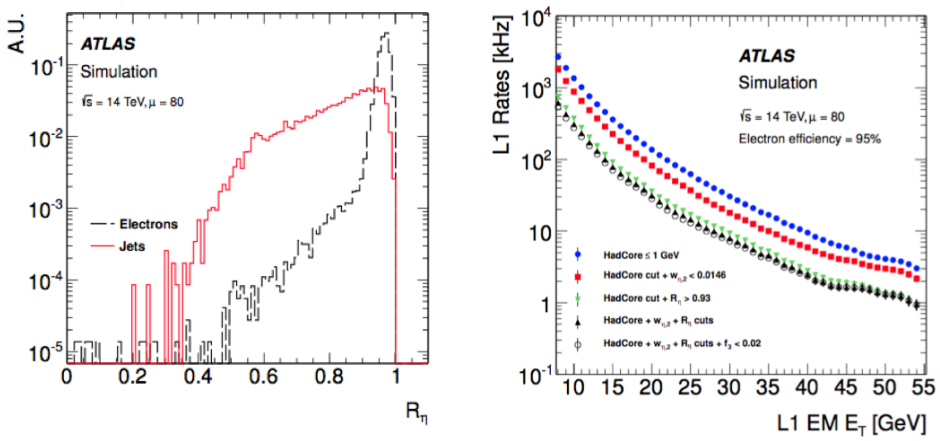

Figure 4: Left: Distributions of the R_η variables (as defined in the text) allowing to distinguish between electrons (black) and jets (red) with $P_T > 20$ GeV. Right: Dependence of the trigger rate on E_T threshold for successive selection criteria considering R_η as well as other shower shape variables.

The existing calorimeter trigger information is based on the concept of a "Trigger Tower" that sums the energy deposition across the longitudinal layers of the calorimeters in a cone of $\Delta\eta \times \Delta\Phi = 0.1 \times 0.1$. The new finer granularity scheme is based on so-called "Super Cells", which provide information for each calorimeter layer for the full η range of the calorimeter, as well as finer segmentation ($\Delta\eta \times \Delta\Phi = 0.025 \times 0.1$) in the front and middle layers of the EM barrel (EMB) and endcap (EMEC) for $|\eta| \leq 2.5$.

The increase in granularity can be seen in Fig. 3, which compares the energy deposition of an electron in the existing trigger readout system to that of the proposed upgrade system.

The finer granularity of the Super Cells, the information on different layers (depth information) and the implemented finer quantization of the energy scale, enable a more sophisticated rejection

of jet backgrounds compared to the current system through the use of shower shape variables. An example is reported in Fig. 4–left where the R_η variable represents the transverse energy measured in the 3×2 Super Cells group divided by the transverse energy measured in a 7×2 group. As shown in Fig. 4–right the use of this variable (along with other shower shape variables) allows a significant jet backgrounds rejection and provides a decrease (by up to a factor of 4 for p_T ∼20 GeV) in the trigger rate for the same electron efficiency.

3.3 New Small Wheel (NSW)

To maintain the capability to trigger on moderate momentum muons under background conditions much harder than those currently present at the LHC, the largest Phase–I upgrade project for the ATLAS Muon System is the replacement of the present first station in the forward regions (the present Small Wheels - SW) with new chambers in the so-called New Small Wheels (NSWs). The primary motivation for introducing the new chambers is to improve the muon tracking performance under the large expected cavern background of neutrons and photons and at the same time improve the rejection of fake muons in the L1 muon trigger by incorporating track-vector information from the NSW. As described in Sect. 2 the muon trigger in the endcap is based on the TGC on the Big Wheel (BW) (after the endcap toroid) which are covering a pseudo-rapidity range of $1.0 < |\eta| < 2.4$. In the BW, track vectors are reconstructed and the momentum, at trigger level, estimated by the bending in the end-cap toroid assuming the particles originated from the interaction point of ATLAS. With this scheme, during Run–1 the forward muon triggers had a very high fake rate (about 90%) due to low energy particles generated in the materials between the SW and the BW, entering the trigger chambers of the BW, as shown in the sketch of Fig. 5–left. The existing ATLAS BW trigger accepts all three tracks shown. The fake tracks (B and C) can be rejected in the trigger by the addition of the NSW which will be covering a η range $1.3 < |\eta| < 2.7$. To further improve the rejection of fake triggers in the full pseudo-rapidity coverage of the BW, hit information of the TGC chambers present in the end-cap inner region (only in the large sectors), and from the energy-loss in the Tile calorimeter in the range $1.0 < |\eta| < 1.3$ will be used already during Run–2 (after the implementation occurred during the consolidation phase in LS1).

The NSW upgrade is designed to cope with the high background rate that is expected at $\mathscr{L} = 2-5\times10^{34}\mathrm{cm}^{-2}\mathrm{s}^{-1}$ during Run–3 and for operation at HL-LHC where background rates as high as ∼ 15kHz/cm^2 can be reached in the most forward region, that cannot be sustained by the MDT in the current SW. In Fig. 5–right the L1 muon trigger rate as a function of the muon p_T threshold, extrapolated to the expected luminosity of 3×10^{34} cm^{-2}s^{-1}, in similar trigger condition of Run–1, after the pre–Phase–I consolidation, and with the presence of the NSW are shown The addition of the NSW will significantly reduce the fake rate contributions allowing deployment of lower muon p_T thresholds at level–1.

The two NSWs consist of eight layers each of Micromegas (MM) and small-strip Thin Gap Chambers (sTGC), both providing trigger and tracking capabilities, for a total active surface of more than 2500 m^2. It represents the first system with such a large size based on Micro Pattern (Micromegas) and wire detectors (sTGC).

The NSW will utilize two detector technologies: small-strip Thin Gap Chambers (sTGC) as the primary trigger and Micromegas (MM) as the primary precision tracker. As shown in Fig. 6(a) following the structure of the present SW, each NSW is composed of 16 sectors (8 small and 8 large)

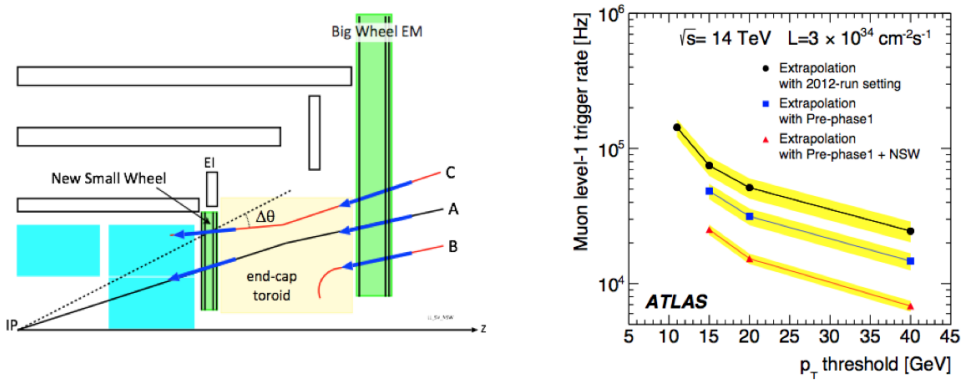

Figure 5: Left: Schematic of the ATLAS muon trigger. The existing Big Wheel trigger accepts all three tracks shown. The fake tracks (B and C) can be rejected in the trigger by the addition of the New Small Wheel. Right: The expected trigger rate of Level-1 muon trigger as a function of pT threshold. The same trigger condition in 2012 (black), the Pre-Phase-I configuration (blue) and the Phase-I configuration with NSW (red).

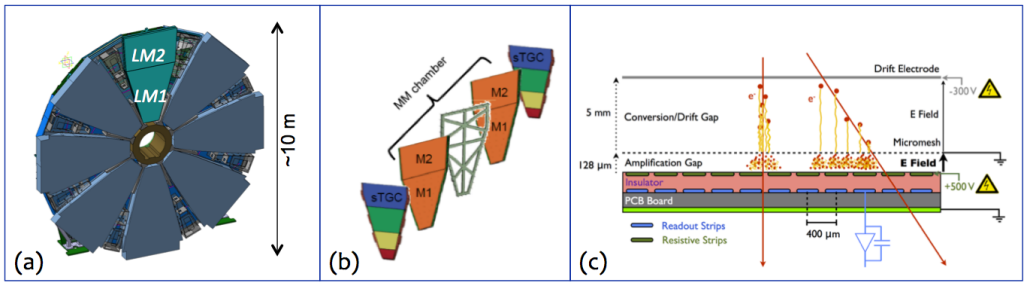

Figure 6: (a): Layout of the New Small Wheel. In one Large sector the TGC 3-modules layer has been cut-out so that the radial segmentation of the MM modules is visible. (b): View of one sector of the wheel. It is composed of a central spacer and a sandwich of MM and sTGC modules. (c): Principle of operation for a resistive MM chamber with readout strips of 400 μm pitch. All dimensions are not to scale.

with a sandwich arrangement of sTGC-MM-MM-sTGC multi-layers in a combination, shown in Fig. 6(b), used to maximize the distance between the two sTGCs multilayers for improved track segment angular resolution at the trigger level. Each sTGC and MM module is a quadruplet, composed by four planes for position measurements in the radial (precision) and in the azimuthal coordinates. For the two wheels (one on each end-cap side of the Spectrometer), the MM and sTGC will cover a total active area of more than 2500 m^2 detector planes. The choice of eight planes per detector was dictated by the need to provide the necessary redundancy for a robust, fully functional detector system over its whole lifetime.

For the first time the MM will be employed in the ATLAS detector, and it represents the first system with such a large surface based on Micro Pattern Gaseous Detectors (MPGD). The principle of operation of this detector is shown in Fig. 6(c). A few mm gap between two parallel electrodes is filled with a gas mixture. The anode is segmented in metallic strips with a pitch of few hundred microns, and above it, at a distance of about 100 μm, determined by special pillars

built on the strip plane, a metallic mesh is deposited and tensioned. The metallic mesh separate the few mm gap drift region (with low electric field) form the thin amplification region. Charged particles traversing the drift space ionize the gas. The electrons liberated by the ionization process drift towards the mesh. Due to the high ratio between the two electric fields, the metallic mesh is essentially transparent for the electrons so that they drift to the mesh, pass in the amplification region, where the avalanche takes place, and finally the signal is collected by the metallic read-out strips. Many years of intensive R&D on ATLAS Micromegas, and major breakthroughs in the technology were necessary to bring the MM to a mature technology, to be approved as one of the components of the NSW [10]. Among them the option to adopt resistive anodes to limit the energy of the discharges in the detectors [11].

3.4 Small Projects for the Muon Spectrometer Upgrade

Other small projects have been proposed for the Phase-I Upgrade after the submission of the Letter of Intent. Among them, the "BIS78" proposal to further improve the fake trigger rejection in the Muon Spectrometer has been recently approved by the Atlas Collaboration Board.

One of the main motivation for the NSW upgrade was to strongly reduce the high rate of fake triggers in the end-cap region and improve the L1 muon momentum selectivity. However this problem will not be completely solved by the NSW which will cover the pseudorapidity range $1.3 < |\eta| < 2.5$, while the barrel-endcap transition region $1.05 < |\eta| < 1.3$, with similar high fake rate and momentum measurements problems, will not be sufficiently instrumented to provide uniform performance offered by the NSW. The fake rate problem can be partially mitigated by exploiting the Tile calorimeter muon signal, which can also be combined in half of the sectors with existing TGC chambers (see Sect. 3.3). For the remaining 50% of the transition region, the BIS78 project proposes to replace the present MDT precision chambers in the extremal regions of the small sectors of the inner barrel layer (Barrel Inner Small - BIS stations 7 and 8) with a new type of muon stations, integrating in the same structure both the new generation of small tubes MDT, the sMDT [12] and the new generation thin RPC [13] with improved performance.

3.5 Atlas Forward Physics (AFP)

The AFP project promises a significant extension to the physics reach of ATLAS by tagging and measuring the momentum and emission angle of very forward protons, that proceed intact along the LHC beam line. This enables the observation and measurement of a range of processes where one or both protons remain intact. Such processes are typically associated with elastic and diffractive scattering, where the proton radiates a virtual colorless object, the so-called Pomeron, which is often thought of as a non-perturbative collection of soft gluons.

Initially included in the Phase-I Upgrade LoI [5], the project originally consisting in two arms, upstream and downstream ATLAS, each arm with stations at 210 and 420 m distance from the interaction point, has evolved such that now it is planned to be limited at the 210 m region.

Each arm of the AFP spectrometer is composed by two tracking stations placed at 8m distance from each other around the 210 m region, and one timing station. The stations are contained in a movable beam pipe (Roman pots) allowing to place the detectors at about 2 mm from the proton beam line during the running phase and to retract them during the injection or beam dump phase.

In Fig. 7 a sketch of the AFP detector layout for the 210 m stations is shown. The beam interface at 204 m contains the first silicon tracking detector. The beam interface at 212 m contains a second, identical, tracking detector followed by the Time-of- Flight detector.

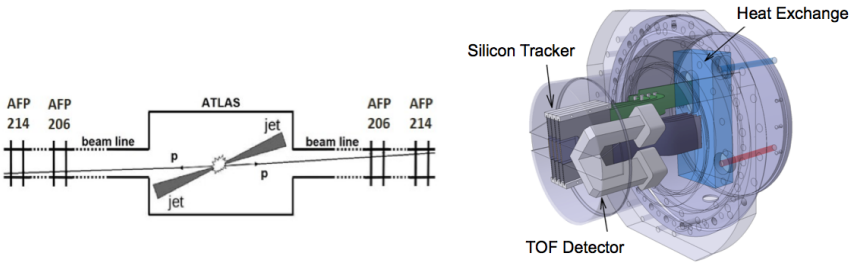

Figure 7: Left: Sketch of the layout of the AFP stations at 204 and 212 m from the ATLAS interaction point. Right: Sketch of the AFP detectors inside a Roman pot

The installation of the AFP detectors is currently foreseen to occur in two phases: a first phase of a single-arm two-station AFP, which does not require timing approved for special low-luminosity runs in Run–2, to be completed, if fully approved, for Phase–I, with the second arm and the timing stations.

4. Phase–II ATLAS Upgrade

The Phase–II upgrade plans have been outlined in the Letter-of-Intent (LoI) submitted in December 2012 [14]. The upgrades will take place during the third long shutdown (LS3) in the transition to the High–Luminosity–LHC where the detectors will be requested to efficiently operate with a peak luminosity of $7 \times 10^{34}\text{cm}^{-2}\text{s}^{-1}$ up to 200 interactions per bunch crossing (pile-up) and a total integrated luminosity of 3000 fb^{-1} collected in about 10 years of operation.

Major upgrades will take place to replace systems due to radiation damage or obsolescence, inability to read-out at the rates available at HL-LHC and to maintain appropriate performance for physics in a very high pile-up environment. Moreover, in order to fully exploit the high luminosity, a significant increase of the hardware trigger rate must be foreseen to maintain thresholds low for specific event topologies, and the event selection for the data acquisition must be improved. This will require replacement of the front-end and back-end read-out electronics of most of the sub-systems, along with some detector upgrades or replacements in the most difficult regions.

The principal components of the ATLAS Phase–II Upgrade are:

- The introduction of a "level–0/level–1" trigger split to enable inclusion of tracking at level–1;
- Full replacement of the inner detector, which cannot handle pile-up above 80 (front-end chips), and will be reaching end-of-life after $\sim$15 years of operation and $\sim$350 fb^{-1} of data;
- Replacement of LAr analogue readout electronics with all-digital system;
- Substantial changes to readout architecture and readout electronics of the muon system.

4.1 Trigger and Data Flow System

The new design of the trigger for Phase–II is based on the splitting of the present (and Phase-I) L1 trigger into two trigger levels, where the Phase–I L1 trigger becomes the Phase–II L0 and the new L1 will include tracking information. This scheme will make use at L0 of improvements made in Phase–I, for example with the NSW and the L1 calorimeter triggers, and it will introduce inner tracking and precision muon information at L1.

After the LoI for the Phase–II upgrade, ATLAS has recently re-evaluated the requirements for the hardware triggers L0 and L1, and last year, agreed to increase the nominal rate limits to 1 MHz for L0 and 400 KHz for L1, with corresponding latency values (nominal/design) of 6/10 μs for L0 and 30/60 μs for L1. The final recorded rate after HLT will be 10 kHz.

For the trigger functionality, the inner tracker will be readout in selected regions (Regions Of Interest) identified by L0 triggers based on calorimeters and muons and participate to L1 tracker trigger. An evolution of the Phase–I FTK system is a good candidate for the L1 track trigger.

4.2 The Atlas Inner Tracker for HL-LHC (ITK)

Tracking detectors play a crucial role in ATLAS, contributing to the identification and reconstruction of particles emerging from the collisions, especially allowing the reconstruction of short-lived particles such as charm and beauty mesons and taus and identifying the vertexes of individual collisions in pile-up events. The present ID was designed to operate 10 years at 1×10^{34} cm^{-2}s^{-1} with a pile-up less than 25 and with trigger rate up to 100 kHz. The main limiting factors at HL-LHC of the present tracker will be: bandwidth saturation (Pixel, SCT); occupancy (TRT, SCT); the radiation damage of the Pixel and SCT detectors, designed for 400 and 700 fb^{-1}, respectively.

To withstand the much harsher radiation and occupancy conditions of the HL-LHC, ATLAS necessitates a complete replacement of the present Inner Detector (ID).

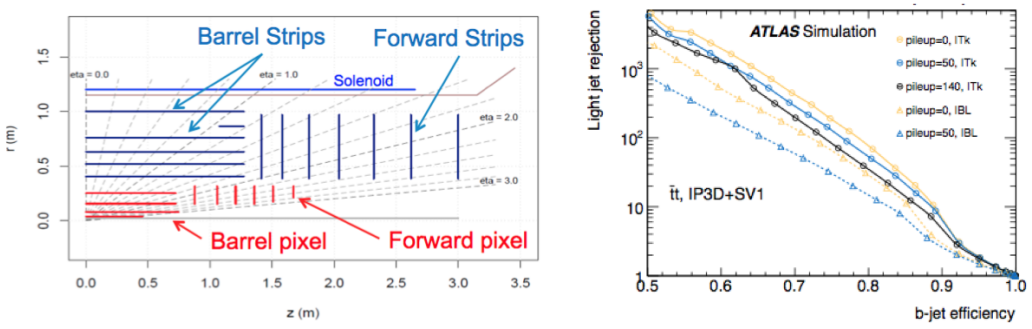

Figure 8: Left: Sketch of the baseline design for the Inner Tracker detector for the Phase–II upgrade; Right: Performance studies for light jet rejection versus *b*–jet efficiency for different numbers of collisions per bunch crossing.

The current baseline design of the Inner TracKer (ITK) is sketched in Fig. 8–left. It is a all silicon detector, with pixel sensors at the inner radii surrounded by microstrip sensors. In the central region, sensors are arranged in cylinders, with 4 pixel layers followed by 3 short-strip layers and 2 long-strip layers. The two end-cap regions are each composed of 6 Pixel and 7 Si-strip double-sided disks, built of rings of modules. The pixel modules are with pixels of sizes 25×150 μm^2

(for the two inner layers) and 50×250 μm^2 (for the two outer layers). Similarly, the Si-strip barrel modules also come in two types, with short strips (24 mm) for the first three layers and long strips (48 mm) for the outmost two layers. As in the current SCT, the Si-strip modules are designed to be of 2 pairs of silicon microstrip sensors, glued back-to-back at an angle of 40 mrad to provide 2D space-points. The proposed design will have a coverage up to $|\eta|$ <2.7 with a total number of 638M channels for the pixels and 74M strips. Intensive R&D studies are also in process to select the most suitable pixel sensor technology out of Si-planar, 3D and diamond, and to find the optimal layout of the Si-strip modules. Other layouts are currently under study, even extending the coverage at larger pseudo-rapidity (for which additional disks in the forward region are under consideration).

The performance of b-tagging, in particular for high energy jets, depends critically on the rate of fake tracks, and on the two-track resolution. In Fig. 8–right, the performance of the current baseline design for light jet rejection versus *b*–jet efficiency of the new tracker is shown for different values of pile-up. Better performance are obtained with ITK at pile-up values up to $\mu = 140$ as compared to the present ID+IBL at $\mu = 0$.

4.3 The Calorimeter System

The Liquid Argon (LAr) calorimeter and the Tile hadronic calorimeter will continue to function at the highest peak luminosities at HL-LHC. Depending on the running conditions and the actual level of radiation, the performance of the forward calorimeter that is located within the end-cap cryostat (FCal), may be degraded due to the increased luminosity. No changes are foreseen on the detectors with the only potential exception of the FCal.

To maintain the FCal functioning at the HL-LHC, two possible solutions are considered [15]: the complete replacement of the FCal, or the installation of a small warm calorimeter, Mini-FCal, in front of the FCal. The Mini-FCal would reduce the ionization and heat loads of the FCal to acceptable levels.

The major upgrade for the calorimeter systems for Phase-II is the full replacement of the front-end and back-end electronics. This is due to both radiation damage and the new requirements of the trigger system, with the latter requiring to provide higher granularity information to the trigger processors and real-time performance capabilities that the current electronics cannot satisfy. The LAr front-end electronics will be upgraded in steps, with the addition of new trigger boards in Phase–I (see Sect. 3.2), and the replacement of the primary read-out and calibration boards in Phase–II. The new read-out architecture will allow full digitization and read-out of data at 40 MHz and transmission to off-detector system, with digital information transfer to the L0/L1 trigger system.

4.4 The Muon System

The Phase–II upgrade for the muon systems are driven by the necessity to maintain low–P_T trigger thresholds, improve the rejection of fake triggers, still maintaining high efficiency, and improve the selectivity for tracks at threshold (sharpen the trigger threshold turn-on curve), which calls for an improved spatial resolution in the bending direction η.

The new trigger system, foreseen for Phase–II, will cause significant discomfort for the "legacy" of on-chamber muon electronics. It will impose new requirements to the trigger readout systems as well as on the precision chambers.

Three are the main issues to solve for running at HL-LHC: operate with the higher trigger rates and longer latencies of the new L0 trigger; integrate the precision chambers in the L0/L1 trigger system for better selectivity; and deal with the high particle flux on the present RPC chambers imposing them to be safely operated at a reduced high-voltage hence at reduced efficiency.

The present readout system of the trigger chambers in the barrel (RPC) and in the end-cap (TGC) will not be able to cope with the new L0/L1 trigger scheme, as the present electronics is designed for maximum latencies of 3.2 μs (TGC) and 6.4 μs (RPC), and for trigger rates up to 100 kHz. Consequently, the whole readout electronics chain will have to be replaced, offering the opportunity to rebuild the readout chain with modern technologies, also exploiting improved capabilities for example with strip charge readout from the RPC for better spatial resolution.

In order to preserve a standalone muon trigger, sharpening of L1 threshold definition is mandatory for Phase-II. This can be accomplished in the end-cap region measuring the direction of the muon before and after the end-cap toroid. The NSW (see Sect. 3.3) is designed to reach 1 mrad angular resolution for the measurement upstream the magnet, while the present trigger system, based on the TGC chambers on the Big Wheel downstream the end-cap toroid, cannot reach the sufficient resolution.

The upgrade foreseen in the end-cap region is to integrate the MDT precision chambers in the L0 trigger, by replacing their readout electronics. The replacement of the MDT readout electronics actually comes from two requirements: for a fast readout chain for a L0 MDT trigger, and to cope with the L1 rate of 400 kHz for the MDT readout. A possible scenario also consider the possibility to partially replace the TGC chambers in the Big Wheel (for the chambers closer to the beam line) with the sTGC (same technology used in the NSW) having a finer granularity and higher spatial resolution.

The need to cope with 400 kHz L1 trigger and the sharpening of the p_T threshold, requires the replacement of MDT readout electronics in the barrel region, as well. However in the barrel there are regions (the inner barrel layer - BI) where it is impossible to access the MDT front-end electronics and its replacement would imply major and long interventions (dismount all the chambers). Different scenarios are currently being considered which, in the case of the choice of only partial replacing of the MDT electronics, could limit the L1 trigger rate to a maximum of 200 kHz. Concerning the trigger chambers in the barrel, the increased background hit rates, will prevent the RPC to work at optimal efficiency. To cope with the possible loss of the efficiency of the trigger, formed by the coincidence of 3 out of 4 RPC stations in the middle and outer layers of the barrel muon system (BM and BO), the proposal to include a third inner layer of RPC coupled to the MDT inner chambers is also currently under evaluation. This proposal has the additional advantage to enhance the trigger coverage in regions not presently covered due to interferences with the supporting structure. The solution to replace, where possible, also the MDT chambers in the barrel inner layer with the new sMDT coupled to this new generation RPC chambers, is certainly an attractive option, which would benefit from the experience of the installation of the same system in a small part of the barrel already planned for the Phase–I (see Sect. 3.4).

5. Conclusions

At the time when LHC is restarting to deliver 13 TeV pp collisions and ATLAS has just com-

pleted its consolidation and maintenance during the first long shutdown, now ready for the next challenging Run-2, ATLAS has planned a coherent upgrade programme from Phase-I up to the High Luminosity-LHC era to fully exploit the LHC energy and instantaneous luminosity at up to 5-7 times the design value. The staged incremental upgrades are strategically designed to maintain flexibility and to fully exploit the physics potential at the LHC.

References

[1] L. Evans and P. Bryant, *LHC Machine*, J. Instr. 3, S0801 (2008).

[2] Proceedings of RLIUP: Review of LHC and Injector Upgrade Plans, Centre de Convention, Archamps, France, 29Ð31 October 2013, edited by B. Goddard and F. Zimmermann, CERN-2014-006 (CERN, Geneva, 2014), http://dx.doi.org/10.5170/CERN-2014-006.

[3] ATLAS Collaboration, *The ATLAS Experiment at the CERN Large Hadron Collider'*, J. Instr. 3, S08003 (2008).

[4] ATLAS Collaboration, *Insertable B-Layer, Technical Design Report*, CERN-LHCC-2010-013.

[5] ATLAS Collaboration, *Letter of Intent for the Phase-I Upgrade of the ATLAS Experiment*, CERN-LHCC-2011-012, LHCC-I-020.

[6] ATLAS Collaboration, *Fast TracKer (FTK) Technical Design Report*, CERN-LHCC-2013-007.

[7] ATLAS Collaboration, *ATLAS Liquid Argon Calorimeter Phase-I Upgrade Technical Design Report*, CERN-LHCC-2013-017.

[8] ATLAS Collaboration, *New Small Wheel Technical Design Report*, CERN-LHCC-2013-006.

[9] ATLAS Collaboration, *Technical Design Report for the Phase-I Upgrade of the ATLAS TDAQ System*, CERN-LHCC-2013-018.

[10] J. Wotschack et al., *The development of large-area micromegas detectors for the ATLAS upgrade*, *Mod. Phys. Lett.* **A 28** (2013) 1340020.

[11] T. Alexopoulos et al., *A spark-resistant bulk-Micromegas chamber for high-rate applications*, *Nucl. Instr. Meth.* **A 640** (2011) 110.

[12] B. Bittner, et al, *Performance of drift-tube detectors at high counting rates for high-luminosity LHC upgrades*, Nucl. Instr. and Meth. A 732 (2013) 250–254

[13] G. Aielli et al., *Studies on fast triggering and high precision tracking with Resistive Plate Chambers*, Nucl. Instr. and Meth A 714 (2013) 115–120
R. Santonico, Introductory talk to the XI workshop on Resistive Plate Chambers and Related Detectors, (2012)

[14] ATLAS Collaboration, *Letter of Intent for thePhase-II Upgrade of the ATLAS Experiment*, CERN-LHCC-2012-022, LHCC-I-023.

[15] J. Turner, *Upgrade Plans for ATLAS Forward Calorimetry for the HL-LHC*, ATL-LARG-PROC-2011-002.